

Study of the beyond standard model interaction using Coherent Elastic Neutrino-Nucleus Scattering process

S. P. Behera^{1,2,*}, S. Panda^{1,2}, and D. K. Mishra^{1,2}

¹*Nuclear Physics Division, Bhabha Atomic Research Centre,
Mumbai - 400085, India and*

²*Homi Bhabha National Institute, Anushakti Nagar, Mumbai - 400094, India*

Phenomenological studies are carried out to find the potential reach of a detector to constraints on possible beyond the standard model general neutrino interactions in the neutrino-quark sector, for the proposed Indian Coherent Neutrino-nucleus Scattering Experiment (ICNSE) at the Bhabha Atomic Research Centre in India. Reactors of different core configuration and power are used as sources of electron antineutrinos. The study has been carried out considering a target mass of 10 kg and an exposure of one year. It has been found that the ICNSE detector has a significant capacity to limit the majority of the Non-standard Interaction(NSI) parameter space. It has also been observed that a combination of results from two different types of detectors such as sapphire and high-purity germanium can significantly improve sensitivity by reducing the degeneracies between some pairs of NSI parameters to a smaller region.

I. INTRODUCTION

The coherent elastic neutrino-nucleus scattering (CE ν NS) process is a low energy phenomenon which has been predicted theoretically in the standard model(SM) more than four decades ago [1]. Now it is well understood in the SM of particle physics. Due to low energy of neutrinos(<100 MeV), the de Broglie wavelength of the scattering process is larger than the nuclear radius ($\lambda = h/q \geq R$, where q refers to the exchanged momentum, R is the nuclear radius). Therefore, the scattering amplitudes on single nucleons add coherently and lead to an enhanced cross section whose value is directly proportional to number of neutrons present in the target nuclei. Despite its large cross section, earlier it has been difficult to observe the CE ν NS process using most conventional high-mass neutrino detectors due to the very small resulting nuclear recoil energies.

Recently, the COHERENT experiment has carried out measurements of the CE ν NS process, utilizing neutrinos produced by an accelerator. They have established this process at a confidence level of 6.7σ using a CsI[Na] scintillator detector [2, 3]. Moreover, they have reported a second measurement conducted with a liquid argon (LAr) detector[4]. The findings reveal that the measured cross section is in agreement with the predictions made by the SM. Additionally, the COHERENT group has achieved a groundbreaking measurement of the CE ν NS process, attaining a significance of 3.9σ with high-purity germanium spectrometers that operate at an energy threshold of 1.5 keV [5]. The measurement of the CE ν NS cross section provides a pathway to explore a variety of physics phenomena across different research fields including particle physics, nuclear physics, astrophysics, and cosmology. Analyzing the CE ν NS process can enhance our understanding of essential physics concepts that extend beyond the SM, such as non-standard interactions [6], the neutrino magnetic moment [7], the weak mixing angle [6, 8–10],

and the distributions of nuclear neutron density [9]. This process also allows for detailed investigations into the interiors of dense objects and stellar evolution [11, 12]. The CE ν NS process not only offers to explore the Beyond Standard Model (BSM) physics but also can be applied for monitoring nuclear reactors. The measurement of CE ν NS process using reactor antineutrinos offers some advantages compared to neutrino produced due to pion-at-rest decay source. Due to low energy(< 10 MeV), the nuclear form factor is almost one at these energies. Furthermore, the possible existence of sterile neutrinos could be confirmed or disproved by using purely electron antineutrinos and observing neutrinos through the flavor-blind (CE ν NS) process. The CE ν NS process was demonstrated by the Dresden-II experiment using electron antineutrinos from a nuclear reactor [13]. Furthermore, the CONUS [14] and CONNIE [15] experiments have established upper limits on CE ν NS that align with the SM predictions, and they are currently working towards their initial detection. Coherent scattering of xenon nuclei in dark matter search initiatives, specifically PandaX-4T [16] and XENONnT [17], has led to the observation of solar neutrinos (8B). There are several experiments are going on and some are underway to measure this process using neutrinos from different sources.

In India, an experimental setup the Indian Coherent Neutrino-nucleus Scattering Experiment(ICNSE) has been proposed to measure the (CE ν NS) cross section using electron antineutrinos produced from reactor and address various fundamental physics aspects. The current study examines the detection capabilities of the ICNSE detector to constrain the possible presence of new type of interaction in beyond the usual V-A structure within the SM called as Non-Standard Interaction(NSI) of neutrinos. The presence of this new interaction creates a diverse phenomenology in both scattering and neutrino oscillation experiments [18]. This is a model-independent framework proposes a new type of contact interactions on the neutrino sector that differs from the electroweak theory in SM. In general, the NSI can be occurred in neutral current and charge current processes. Both possibilities propose the existence of new kind of mediator that carries heavier mass or in the same order with the electroweak counterparts.

* shiba@barc.gov.in

Regarding the $\text{CE}\nu\text{NS}$ process, only the neutral current case is concerned. Neutrino within NSI framework affects quark constituent of a nucleus, which can be occurred as non-universal flavor conserving or flavor violating process. The examination of sensitivity to the NSI parameters is significant that helps understanding neutrino properties, as any affirmative signal may indicate the presence of new physics BSM. The potential presence of neutrino NSIs may impact neutrino oscillation rates, enhance our understanding of how neutrino masses are generated, and open up new paths for exploring dark matter and cosmological physics. Conversely, limitations imposed on these parameters could potentially eliminate certain models of new physics.

The paper is structured as follows. In the following section, a detailed design concept of the proposed ICNSE setup is presented. The $\text{CE}\nu\text{NS}$ process both within the SM and in presence of NSI is discussed in Sec. III. The simulation method for estimating expected number of events in the detector is described in Sec. IV. The procedure for finding the sensitivity of the proposed experiment is described in Sec. IV A. The sensitivity of detector to NSI parameters for an exposure of one year is elaborated in Sec. V. In Sec. VI, observations obtained from this study is summarized and discussed the implication of this work.

II. THE PROPOSED ICNSE SETUP

Experiments based on the $\text{CE}\nu\text{NS}$ process demand detectors that operate at very low threshold energy, which are vital for measuring nuclear recoil energies that are typically in the few keV range. Semiconductor detectors made from germanium or silicon are suitable candidates for meeting these low threshold requirements. However, the energy thresholds of these detectors are generally around the keV level, which is still too high to effectively observe the $\text{CE}\nu\text{NS}$ process with reactor antineutrinos. Cryogenic detectors present a viable solution, as they can achieve both low thresholds and excellent energy resolution. These detectors can be fabricated from various materials, including semiconductors like germanium and insulators such as calcium tungstate and sapphire (Al_2O_3). However, sapphire is an excellent candidate for observing $\text{CE}\nu\text{NS}$ because of the lower atomic masses of Al and O , which enhances sensitivity to lower nuclear recoil energies. Sapphire has favorable phononic characteristics, and it has already been demonstrated that low-energy thresholds $\mathcal{O}(0.1\text{keV})$ are achievable with these crystals. A baseline recoil energy resolution of 18 eV, which corresponds to a recoil energy threshold of 54 eV, has been accomplished using a newly developed 100 g sapphire detector [19]. According to a sensitivity analysis conducted in Ref. [20], the $\text{CE}\nu\text{NS}$ process can be detected at a 5σ level with cryogenic detectors that have recoil energy thresholds of 20 eV. Therefore, in this work, only sapphire has been utilized as the target material. The conceptual design of the detector setup has been derived from Ref. [21]. The detector design includes the multilayered structure of shielding materials for reducing both natural and reactor related background. The method of signal extraction

from the detector is described in Ref. [22] and list of references mentioned there.

III. THEORETICAL MODEL ON INTERACTION PROCESS

The relevant cross sections for $\text{CE}\nu\text{NS}$ process both within and beyond the SM scenario under consideration is presented here. In the following section the SM cross sections has been discussed followed by the cases of Neutrino Non-standard Interaction (NSIs), and Neutrino Generalized Interaction (NGIs).

A. The standard model $\text{CE}\nu\text{NS}$ cross section

In the SM, the differential $\text{CE}\nu\text{NS}$ scattering cross section is given by

$$\frac{d\sigma}{dT}(E_\nu, T) = \frac{G_F^2}{2\pi} Q_W^V{}^2 \times A \left(2 - \frac{TA}{E_\nu} \right) |F(q)|^2. \quad (1)$$

In Eq. 1, A , N , Z are the mass of nucleus, number of neutrons, and number of protons in the nucleus, respectively. The SM weak charge is expressed as

$$(Q_W^V)^2 = (g_p^V Z + g_n^V N)^2. \quad (2)$$

In Eq. 2, g_p^V and g_n^V are corresponding coupling of proton and neutron, respectively to Z^0 boson. The coupling terms are expressed through weak mixing angle $\sin^2\theta_W = 0.2386$ by the relation given by $g_p^V = 1/2 - 2\sin^2\theta_W$ and $g_n^V = -1/2$. Further, E_ν is the incident neutrino energy, T is nuclear recoil energy, $(T_{\max}(E_\nu) = 2E_\nu^2/(A + 2E_\nu))$, G_F is the Fermi coupling constant, θ_W is the weak mixing angle, and $F(q)$ is the nuclear form factor for a momentum transfer of q (~ 1.0 at low q).

B. The Neutrino Non-standard Interaction

The $\text{CE}\nu\text{NS}$ process modifies due to the presence of the NSI of neutrinos and quarks. At low energies ($\ll M_Z$), the vector-type neutrino NSI with u and d quarks can be described by the effective Lagrangian

$$\begin{aligned} \mathcal{L}_{\nu\text{Hadron}}^{NSI} = & -\frac{G_F}{\sqrt{2}} \sum_{\substack{q=u,d \\ \alpha,\beta=e,\mu,\tau}} [\bar{\nu}_\alpha \gamma^\mu (1 - \gamma^5) \nu_\beta] \times \\ & \left(\varepsilon_{\alpha\beta}^{qL} [\bar{q} \gamma_\mu (1 - \gamma^5) q] + \varepsilon_{\alpha\beta}^{qR} [\bar{q} \gamma_\mu (1 + \gamma^5) q] \right), \end{aligned} \quad (3)$$

where $\varepsilon_{\alpha\beta}^{qP}$ ($q = u, d$ and $P = L, R$) describe the NSI parameter, both for the non-universal terms, $\varepsilon_{\alpha\alpha}^{qP}$, as well as for the flavor-changing contributions, $\varepsilon_{\alpha\beta}^{qP}$ ($\alpha \neq \beta$). Parameters ε

measure the strength of interaction in analogous to Fermi theory that is given by $\varepsilon \sim \frac{g_X^2}{g^2} \frac{M_W^2}{M_X^2}$, where M_X and g_X are the mass and coupling strength of a heavy mediator. Due to this new type of interaction with heavy mediator, the weak charge is replaced by corresponding NSI charge that is expressed as

$$(Q_{NSI}^V)^2 = [(2\varepsilon_{\alpha\alpha}^{uV} + \varepsilon_{\alpha\alpha}^{dV} + g_p^V) Z + (\varepsilon_{\alpha\alpha}^{uV} + 2\varepsilon_{\alpha\alpha}^{dV} + g_n^V) N]^2 + \sum_{\alpha \neq \beta} [(2\varepsilon_{\alpha\beta}^{uV} + \varepsilon_{\alpha\beta}^{dV}) Z + (\varepsilon_{\alpha\beta}^{uV} + 2\varepsilon_{\alpha\beta}^{dV}) N]^2 \quad (4)$$

where $\varepsilon_{\alpha\beta}^{qV} \equiv \varepsilon_{\alpha\beta}^{qL} + \varepsilon_{\alpha\beta}^{qR}$. Also it can be observed from the above Eq. 4 that degeneracies arising when two NSI parameters are assumed to be non-vanishing at a time. In the above Eq. 4 by setting the ε to zero leads to the SM CE ν NS. In this study the neutral current NSI of neutrinos with the vector couplings has been considered. Currently, the focus is on investigating the potential for NSI arising from electron anti-neutrinos, as the muon NSI parameters are typically more constrained by other experiments. Then considering the above mentioned reason, the NSI interaction due to electron anti-neutrino, Eq. 4 is modified as

$$(Q_{NSI}^V)^2 = [(2\varepsilon_{ee}^{uV} + \varepsilon_{ee}^{dV} + g_p^V) Z + (\varepsilon_{ee}^{uV} + 2\varepsilon_{ee}^{dV} + g_n^V) N]^2 + [(2\varepsilon_{e\tau}^{uV} + \varepsilon_{e\tau}^{dV}) Z + (\varepsilon_{e\tau}^{uV} + 2\varepsilon_{e\tau}^{dV}) N]^2. \quad (5)$$

The NSI interaction cross section can be obtained by replacing Q_W^V by Q_{NSI}^V in Eq. 1. The constrain on parameters $\varepsilon_{\alpha\beta}$ due to the interaction of electron and muon type neutrinos with quarks are summarized in Ref. [23]. It has been observed that both ε_{ee} and $\varepsilon_{e\tau}$ are poorly constrained. Therefore, in this study it is focused on constraining both ε_{ee} and $\varepsilon_{e\tau}$.

C. Neutrino generalized interaction

In addition to the previously mentioned normal effective vector-type NSI framework, more exotic BSM interactions with non-standard Lorentz structures, such as scalar, tensor, pseudoscalar, or axialvector couplings, may be feasible. These interactions are treated as neutrino generalized interactions (NGIs) and considered in the evaluation of the detector's sensitivity. An effective Lagrangian for heavy mediators can be described as [24]

$$\mathcal{L}_{NC}^{\text{NGI}} \supset \frac{G_F}{\sqrt{2}} \sum_{X=(S,V,T)} \mathcal{Q}_X (\bar{\nu}_e \Gamma^X P_L \nu_e) (\bar{\mathcal{A}} \Gamma_X \mathcal{A}), \quad (6)$$

where, $\Gamma^X = \{\mathbb{I}, \gamma^\mu, \sigma^{\mu\nu}\}$ for scalar, vector and tensor type interaction respectively. $\sigma^{\mu\nu} = \frac{i}{2}[\gamma^\mu, \gamma^\nu]$ and $P_L \equiv (1 - \gamma^5)/2$ is the left-handed projection operator. The \mathcal{A} in the expression shows the nucleus.

The NGI can contain the pseudo-scalar and axial-vector parts. However, the contributions do not yield observable effects in current experimental sensitivities $\left[\mathcal{O} \left(\frac{T_N}{m_N} \right) \right]$ and

axial-vector interactions do not coherently sum over heavy spin-zero nucleons. This results in negligible contributions to CE ν NS cross-section. Although spin-dependent interactions can arise from nuclei with nonzero spin such as aluminum-27 in a sapphire detector. In this study we have omitted both pseudoscalar and axial-vector interactions.

The parameter \mathcal{Q}_X in Eq. (6) represents the effective coupling between neutrinos and nuclei for scalar ($X = S$), vector ($X = V$) and tensor ($X = T$) type interactions. These couplings determine the contribution of neutrino generalized interactions to the CE ν NS cross section, which takes the form:

$$\left. \frac{d\sigma_{\nu\mathcal{A}}}{dT_{\mathcal{A}}} \right|_{\text{CE}\nu\text{NS}}^{\text{NGI}} = \frac{G_F^2 A}{\pi} F_W^2(|\mathbf{q}|^2) \left[\mathcal{Q}_S^2 \frac{AT_{\mathcal{A}}}{8E_\nu^2} + \left(\frac{\mathcal{Q}_V}{2} + \mathcal{Q}_V^{\text{SM}} \right)^2 \left(1 - \frac{AT_{\mathcal{A}}}{2E_\nu^2} - \frac{T_{\mathcal{A}}}{E_\nu} \right) \right]. \quad (7)$$

In the above Eq. 7, the scalar and vector charges can be expressed as follows

$$\mathcal{Q}_S = C_{\nu S} \sum_{q=u,d} C_{qS} \left(Z \frac{m_p}{m_q} f_{T_q}^{(p)} + N \frac{m_n}{m_q} f_{T_q}^{(n)} \right), \quad (8)$$

$$\mathcal{Q}_V = \phi C_{\nu V} [Z(2C_{uV} + C_{dV}) + N(C_{uV} + 2C_{dV})]. \quad (9)$$

Here, $m_u = 2.2\text{MeV}$ and $m_d = 4.7\text{MeV}$ are the masses of up and down quarks, respectively [25]. Also, m_p and m_n represent the masses of proton and neutron, respectively. The value of parameter ϕ , depends on the choice of model, however in this study it is considered as $\phi = 1$. The coefficients $f_{T_q}^{(p)}$ and $f_{T_q}^{(n)}$ represent the contributions of the quark mass to the nucleon mass. The values these parameters is taken as follows:

$$f_{T_u}^p = 0.026, \quad f_{T_d}^p = 0.038, \\ f_{T_u}^n = 0.018, \quad f_{T_d}^n = 0.056.$$

In this analysis, we have not treated the ν -quark coupling explicitly, rather taken it in a way of quark-dependent coupling, which is defined by $C_X^q = \sqrt{C_{\nu X} \cdot C_{qX}}$. The scalar and vector contributions are presented separately, as well as in a mixed configuration. At an energy scale below electroweak scale, it is natural to consider an effective field theory approach. Tensor interactions, having a different chiral structure, do not interfere with the SM amplitude and can be encoded in an effective nuclear charge analogous to the weak charge. In this case we can address the tensorial interaction in the model independent $\epsilon_{\alpha\beta}^{qT}$ space considered from Ref. [26] and defined as

$$\mathcal{Q}_T = Z(2\epsilon_{\alpha\beta}^{uT} + \epsilon_{\alpha\beta}^{dT}) + N(\epsilon_{\alpha\beta}^{uT} + 2\epsilon_{\alpha\beta}^{dT}) \quad (10)$$

where “ α, β ” represent the lepton flavor. For this analysis only electron flavor sensitivity is considered, i.e. $\epsilon_{ee}^{uT} - \epsilon_{ee}^{dT}$. It can be noted from Eq. 10 that the proton number does not receive a minor prefactor weighting. Therefore, the cross-section does not inherently correlate with the characteristic dependence on

the squared neutron number as in the case of the SM CE ν NS process. In this study the focus is to constraint both ε_{ee}^{uT} and ε_{ee}^{dT} . The procedure for estimating the expected number of events in the detector as well as the possible sensitivity of the detector to NSIs parameters that the proposed experiments can reach are described in the next section.

IV. SIMULATION METHOD FOR ESTIMATING THE EXPECTED EVENT RATE AND EXTRACTION OF THE DETECTOR SENSITIVITY

Event rate has been estimated considering detection energy threshold of 100 eV, 80% of the detection efficiency independent of nuclear recoil, 90% fiducial volume of the detector, 70% reactor duty cycle and, for an exposure of one year. Studies have been conducted using a target mass of 10 kg to extract the detector sensitivity for various parameters related to neutrinos NSI process. The number of events expected in the sapphire detector due to various reactor power as well as reactor core to detector distance has been estimated using the CE ν NS process and mentioned in Ref. [22]. The number of event expected in the detector due to CE ν NS process has been estimated using Monte Carlo simulation method. The procedure for finding the event in detector is mentioned below

$$N^{\text{events}} = \epsilon t f_0 \frac{M_{\text{detector}}}{A} \int_{E_{\nu\text{min}}}^{E_{\nu\text{max}}} f(E_{\nu}) dE_{\nu} \int_{T_{\text{min}}}^{T_{\text{max}}(E_{\nu})} \left(\frac{d\sigma}{dT} \right) dT, \quad (11)$$

where M_{detector} is the mass of the detector, t is the time duration of data taking, f_0 is the total neutrino flux, $f(E_{\nu})$ is the neutrino spectrum and, ϵ is the efficiency of detector. The production mechanism of $\bar{\nu}_e$ produced from a reactor is discussed in Ref. [21]. The minimum recoil energy of the nuclei in a specific experimental setup is determined by the detector threshold. Since there are fewer neutrinos with higher energy, we have chosen to analyze neutrinos with a maximum energy of approximately 6.0 MeV. Initially, it is planned to use Apsara-U research reactor facility at Bhabha Atomic Research Centre (BARC), India [27] as a source for $\bar{\nu}_e$ s. The Apsara-U reactor's primary benefit is its small and movable core. One advantage of using a movable core is that position-specific observations may be used to cancel systematic errors related to the reactor and detector. In the later stage the same detector setup can be used in other reactor facilities, including Dhruva, BARC [28], proto-type fast breeder reactor (PFBR) [29], IGCAR, Kalpakkam, and VVER, Kudankulam in India [30], might eventually have the same detector configuration. Table I provides information on reactor thermal power, core sizes, and fuel compositions. The comparison of recoil event rate due to various types of detector placed at 4 m distance from Apsara-U reactor is shown in Fig. 1. Event rates are obtained considering $\varepsilon_{ee}^{uV} = \varepsilon_{ee}^{dV} = \varepsilon_{\tau e}^{uV} = \varepsilon_{\tau e}^{dV} = 0.1$. In the case of detector made up of Ge the event rate due to NSI is more compared to event rate due to SM CE ν NS process. The increase in event rate is due to the NSI charge Q_{NSI}^V .

It is found that the presence of non-zero NSI can increase or reduce the event rate as shown in left panel of Fig. 1. This observation shows that the NSI phenomenon is a good candidate to extract new physics from the BSM phenomenon.

A. Extraction of the Detector Sensitivity

This study aims to evaluate the capabilities of the ICNSE detector in measuring NSI parameters through the use of $\bar{\nu}_e$ s produced from different reactor facilities, as outlined in Table I. The parameterization of the $\bar{\nu}_e$ s flux due to various fuel compositions of different reactors is detailed in Ref. [21]. These $\bar{\nu}_e$ s are resulting from the beta decay of fission fragments, specifically focusing on energy spectra above 2.0 MeV and the corresponding parameterization has been considered from Ref. [31, 32]. Similarly, the low energy $\bar{\nu}_e$ s produced due to fission has been considered and it is mentioned in Ref. [21]. Further, $\bar{\nu}_e$ s produced due to thermal neutron capture by the ^{238}U exhibit energies below 2 MeV, and corresponding numerical data for this segment of the spectrum has been sourced from Ref. [33]. To assess the detector's sensitivity to NSI parameters, the analysis presumes that an experiment aimed at detecting CE ν NS events will align with the SM predictions. Any discrepancies would suggest the existence of a new physics. A statistical analysis is conducted to compare the predicted event distributions from simulations with the expected distributions, thereby quantifying the detector's sensitivity for a specific exposure. The sensitivity to various parameters is subsequently determined by calculating the χ^2 value. The definition of χ^2 is taken from Ref. [34] and given as

$$\chi^2 = \frac{[(1 + \xi)N^{th}(\xi) - N^{ex}]^2}{\sigma_{\text{stat}}^2 + \sigma_{\text{sys}}^2} + \frac{\xi^2}{\sigma_{\xi}^2}, \quad (12)$$

where ξ denotes the pull parameter with uncertainty σ_{ξ} . In Eq. 12, N^{ex} , N^{th} are representing the number of events obtained from the simulations with the deviation from SM CE ν NS cross section (considered as measured) and with consideration of the SM CE ν NS cross section (considered as theoretically predicted) events, respectively. The procedure for estimating theoretically predicted events N^{th} with consideration of reactor as well as detector related parameters is mentioned earlier. In both types of simulated events, detector response such as resolution and efficiency are incorporated. The procedure for detector response incorporation is mentioned in Ref. [21]. The statistical uncertainty σ_{stat} and the systematic uncertainty σ_{sys} of the event number in the recoil energy bin are given by

$$\sigma_{\text{stat}} = \sqrt{N^{th} + N_{\text{bkg}}}, \quad \sigma_{\text{sys}} = \sigma_{\alpha}(N^{th} + N_{\text{bkg}}) \quad (13)$$

Here N_{bkg} is the number of background events. We assume that σ_{sys} is proportional to the event number with a coefficient σ_{α} . The χ^2 is minimized with respect to pull variables ξ and it is estimated by considering different sources of systematic uncertainties. It includes normalization uncertainty

TABLE I. Various types of reactors used as $\bar{\nu}_e$ sources

Reactors name	Thermal power(MW _{th})	Fuel type	Core sizes, R: radius, H: Height
Apsara-U	2.0	U ₃ Si ₂ -Al (17% enriched ²³⁵ U)	R = 0.32 m, H = 0.64 m
Dhruva	100.0	Natural uranium (0.7% ²³⁵ U)	R = 1.5 m, H = 3.03 m
PFBR	1250.0	MOX(PuO ₂ -UO ₂)	R = 0.95 m, H = 1.0 m
VVER	3000.0	UO ₂ (3.92 % enriched ²³⁵ U)	R = 1.58 m, H = 3.53 m

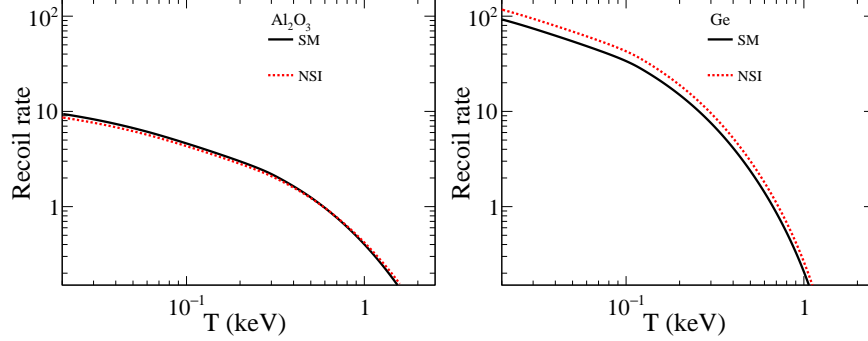


FIG. 1. Recoil event rate of various detectors such as Al_2O_3 (left panel) and Ge(right panel) place at 4m distance from Apsara-U reactor. The rate has been estimated for an exposure of one day with target mass of one 1 kg.

which arises due to reactor total neutrino flux, number of target atoms, and detector efficiency, uncertainty due to nonlinear energy response of the detector, and uncertainty in the energy calibration. So an overall $\sigma_\xi = 5\%$ systematic uncertainty has been considered. The measurement of low energy of recoil nuclei from the CE ν NS process faces a significant challenge due to the presences of both natural and reactor backgrounds such as gamma-rays and neutrons. The detector's sensitivity is affected by both the types of backgrounds and their energy-dependent configuration. At low recoil energy, two distinct background shapes are observed: the $1/T$ shape and flat-shaped backgrounds, as referenced in Ref. [35]. Similarly the systematic uncertainty due to backgrounds is considered as $\sigma_f = 5\%$. At different signal-to-background ratio has been taken into consideration to determine the sensitivity of the detector in the presence of background. In the following sections, the sensitivity of sapphire detectors to NSI parameters is discussed.

V. RESULTS AND DISCUSSIONS

In this section the potential sensitivity of the detector to NSI and NGI parameters coming from the coherent neutrino-nuclei scattering process is presented. It has been assumed a target mass of 10 kg and an exposure of 1 year, considering both absence and presence of background and with electron antineutrinos as a probe. In the case of NSI, three different cases are studied such as non universal flavor conserving, flavor changing and a combination of both while limiting the corresponding parameters. The signature of NSI can be inferred due to a deviation from the expected SM cross section. Similarly, the sensitivity of the detector due to different NGI

parameters such as scalar, vector and tensor are discussed below.

A. Sensitivity of the detector to non-universal NSI parameters

The potential reach of the detector has been extracted considering of only non-universal parameters. The constraint on NSI parameters obtained considering the interaction of neutrinos with both u- and d-type quarks. Figure 2 shows expected allowed region in $\varepsilon_{ee}^{dV} - \varepsilon_{ee}^{uV}$ plane at 90% C.L. for a sapphire detector considering the antineutrino produced from various reactors as mentioned earlier. The sensitivity of the detector has been obtained considering without and with presence of background and for the latter case a signal-to-background ratio is considered as 1.0. It is found that both u- and d-types NSI parameters are strongly correlated. The behavior of this results can be explained considering the expressions of the weak nuclear charge due to the SM CE ν NS process and the weak charge due to the NSI that leads to different event rates. Total number of expected events can be estimated by considering ε_{ee}^{uV} and ε_{ee}^{dV} as mentioned below

$$N^{th} = [Zg_V^p + Ng_V^n + (A + Z)\varepsilon_{ee}^{uV} + (A + N)\varepsilon_{ee}^{dV}] \quad (14)$$

where the slope of the curve on the plane $(\varepsilon_{ee}^{uV}, \varepsilon_{ee}^{dV})$ is described by the ratio $m = (A + N)/(A + Z)$. Due to the above relation mentioned in Eq. 14, allowed regions of Fig. 2 appear as a linear band in the $\varepsilon_{ee}^{uV} - \varepsilon_{ee}^{dV}$ plane. It has been also found that detector sensitivity is almost independent of reactor core configuration and the power of the reactor. Further, a more stringent limit on coupling parameters can be placed by performing the experiment with a combination of target materials [36]. It is also be seen from above that more

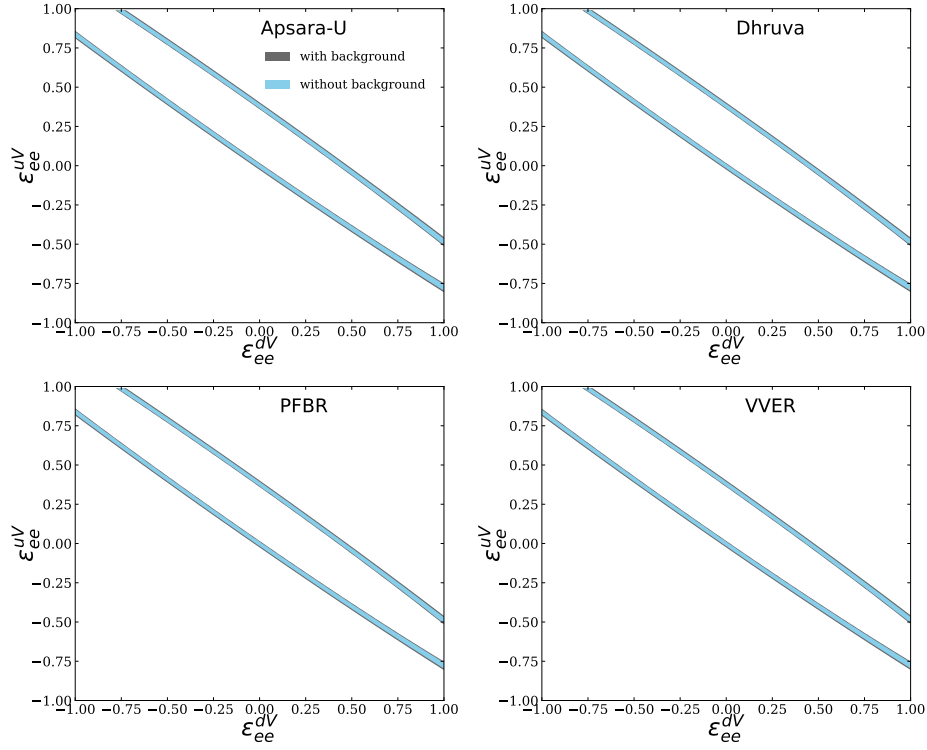


FIG. 2. The allowed regions of non-universal NSI parameters ε_{ee}^{uV} - ε_{ee}^{dV} plane at 90% C.L. considering the Apsara-U, Dhruva, PFBR and, VVER reactors as antineutrinos sources.

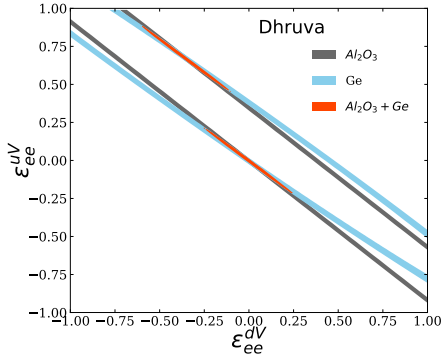


FIG. 3. An expected allowed regions of non-universal NSI parameters ε_{ee}^{uV} - ε_{ee}^{dV} plane at 90% C.L. considering detector made up with Al_2O_3 and Ge. Orange shaded region shows the combined results. Results are extracted considering a signal-to-background ratio of 1.

$(A + N)/(A + Z)$ ratio differs between the two targets, the better stringent limits can be obtained. In this study high purity germanium detector also has been considered. It has been assumed that the procedure for signal extraction from the detector is same as the sapphire detector. Figure 3 shows the excluded region considering targets of Al_2O_3 and Ge, each one has mass of 5 kg and with consideration of a signal-to-background ratio of 1.0. It can be noted here that, total mass as well as exposure have been kept as same while considering a combination of target materials. Gray and light-blue

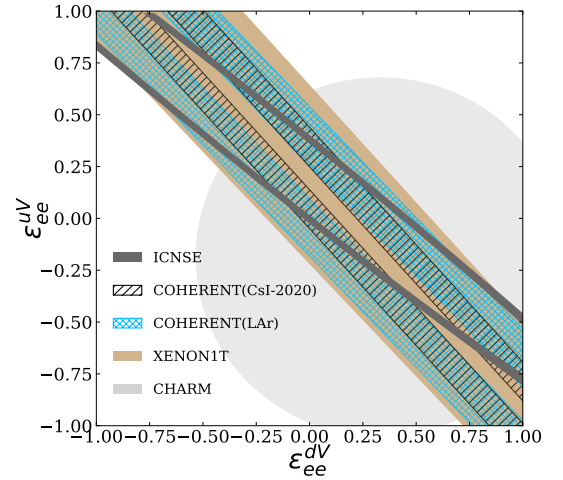


FIG. 4. In the ε_{ee}^{uV} - ε_{ee}^{dV} plane at 90% C.L. comparisons of sensitivity of ICNSE detector placed at 10 m from Dhruva reactor with others experimental observations.

shaded portion show the sensitivity of individual Al_2O_3 and Ge detector, respectively for an exposure of one year. Orange shaded region shows the combined results that improves the sensitivity of detector and minimizing the degeneracy in the parameter space. A similar improvements in sensitivity has been found while placing the detector at other reactor facilities. Figure 4 shows the comparison between the expected

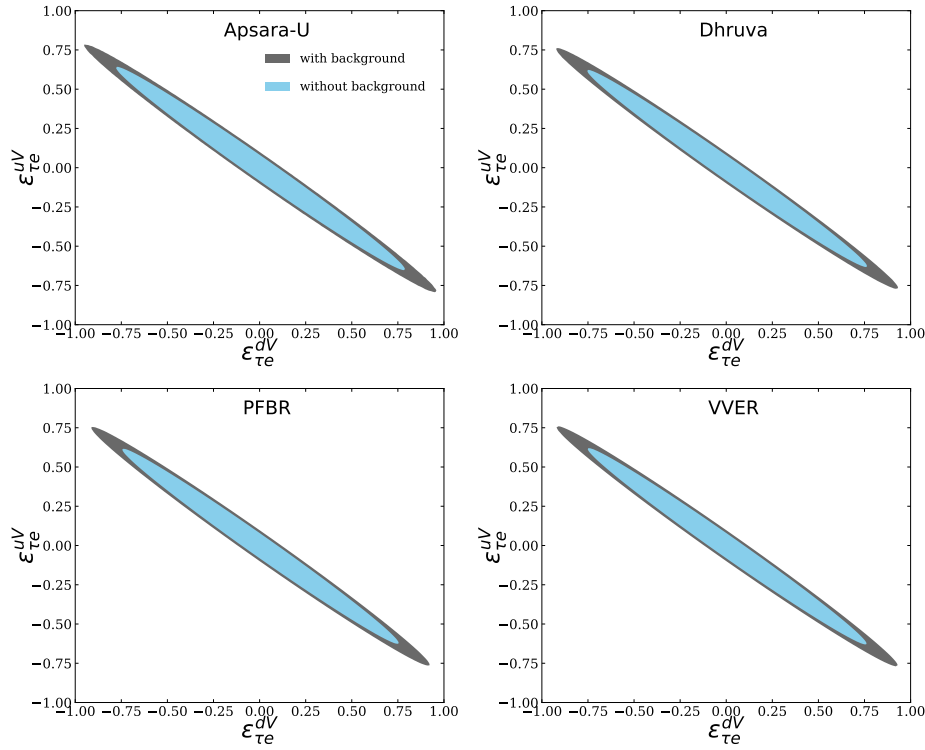


FIG. 5. The allowed regions of flavor changing NSI parameters $\varepsilon_{\tau e}^{uV}$ - $\varepsilon_{\tau e}^{dV}$ plane at 90% C.L. considering Apsara-U, Dhruva, PFBR and, VVER reactors as antineutrinos sources.

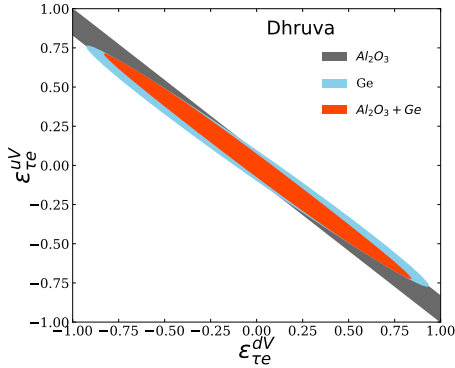


FIG. 6. An expected allowed regions of non-universal NSI parameters in $\varepsilon_{\tau e}^{dV}$ - $\varepsilon_{\tau e}^{uV}$ plane at 90% C.L. considering detector made up with Al_2O_3 and Ge. Orange shaded region shows the combined results. Results are extracted considering a signal-to-background ratio of 1.0.

sensitivity of the ICNSE sapphire detector placed at 10 m from Dhruva reactor core and other experimental observations such as results from CsI [3] and LAr [4] detectors of the COHERENT, XENON1T [37], and CHARM [38] groups. It is found that the sensitivity of ICNSE detector is comparable with other and can put a stringent limit in the parameter space.

B. Sensitivity of the detector to flavor changing NSI parameters

The sensitivity of the detector has been evaluated with a focus on flavor-changing neutrino NSI parameters, specifically excluding non-universal terms. In particular, parameters like $\varepsilon_{\tau e}^{uV}$ and $\varepsilon_{\tau e}^{dV}$ are considered, as there are strong constraints on $\varepsilon_{\mu e}^{uV}$ and $\varepsilon_{\mu e}^{dV}$ due to findings from $\mu - e$ conversion on nuclei [39]. Figure 5 illustrates the expected performance of a sapphire detector in the $\varepsilon_{\tau e}^{dV} - \varepsilon_{\tau e}^{uV}$ parameter space, expressed at a 90% confidence level, both when background present and when it is absent. It is notable that the detector's sensitivity is reduced when background noise is present. As previously explained, enhancing detector sensitivity can be achieved by utilizing targets made from combination of low and high Z materials. Figure 6 shows a comparison of detector sensitivity when using targets made up of Al_2O_3 and Ge each one has mass of 5 kg. It has been observed that a detector made up from Ge exhibits superior sensitivity compared to one made from Al_2O_3 . Moreover, the orange shaded area represents allowed regions from combined analysis of results from both the detector that collectively boosts sensitivity while reducing parameter space degeneracy. This approach effectively optimizes detection capabilities, offering a clearer understanding of material-based sensitivity differences in detectors.

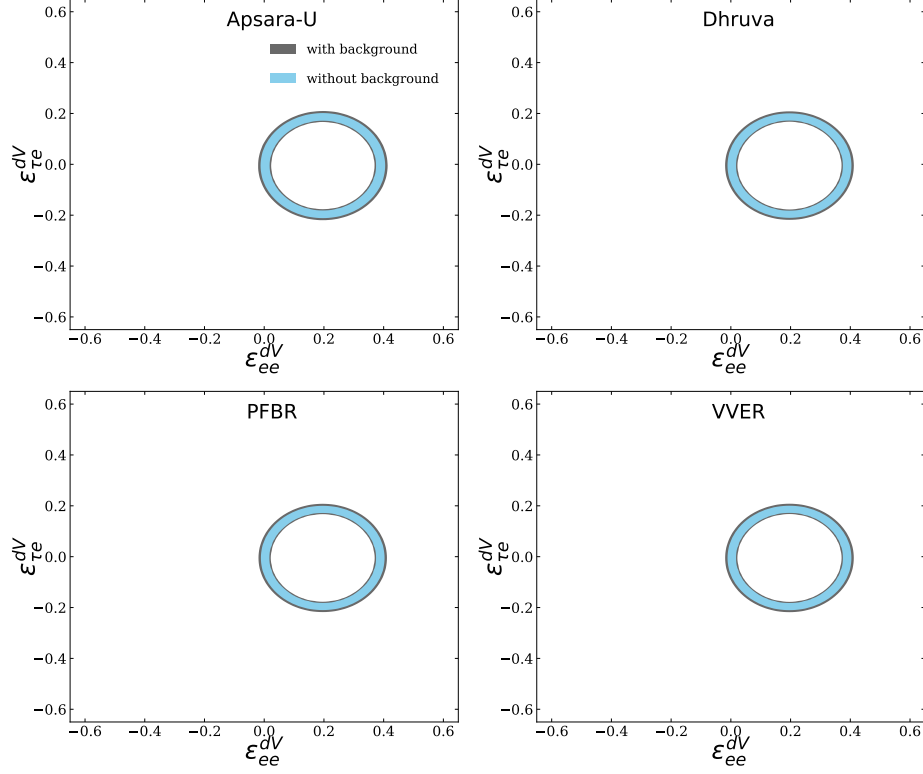


FIG. 7. The allowed regions of non-universal and flavor changing NSI parameters ε_{ee}^{dV} - $\varepsilon_{\tau e}^{dV}$ plane at 90% C.L. considering Apsara-U, Dhruva, PFBR and, VVER reactors as antineutrinos sources.

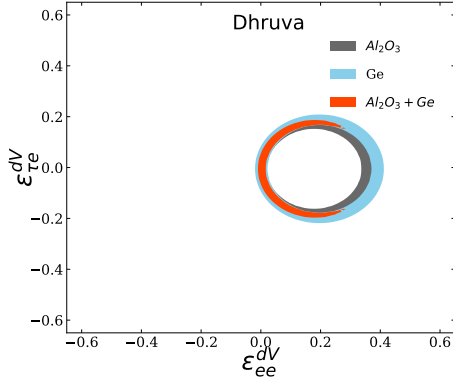


FIG. 8. An expected allowed regions of non-universal NSI parameters ε_{ee}^{dV} - $\varepsilon_{\tau e}^{dV}$ plane at 90% C.L. considering detector made up with Al_2O_3 and Ge. Orange shaded region shows the combined results. Results are extracted considering a signal-to-background ratio of 1.0

C. Sensitivity of the detector to both non-universal and flavor-changing NSI parameters

The potential of a detector has been extracted considering non-universal and flavor changing NSI parameters one at a time, for NSI with d-type quark only. In this case ε_{ee}^{dV} and $\varepsilon_{e\tau}^{dV}$ are considered to be non-zero for which $\bar{\nu}_{e\tau}$ are affected (considering ε_{ee}^{uV} and $\varepsilon_{e\tau}^{uV} = 0$). The ex-

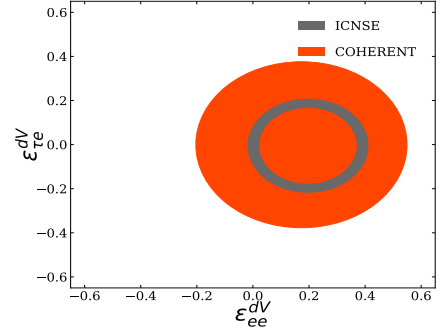


FIG. 9. Comparison of sensitivity of 10 kg Al_2O_3 detector at an exposure of one year with other experimental observations in the ε_{ee}^{dV} - $\varepsilon_{\tau e}^{dV}$ plane at 90% C.L. The detector is placed at 10 m from Dhruva reactor core and with consideration of expected signal-to-background ratio of one.

pected allowed region is between two circles as shown in Fig. 7 at 90 % C.L. considering sapphire detector without and with presence of background. The expected region can be understood by using the relation $(Zg_p^V + Ng_n^V)^2 = [Z(g_p^V + \varepsilon_{ee}^{dV}) + N(g_n^V + 2\varepsilon_{ee}^{dV})]^2 + [Z\varepsilon_{e\tau}^{dV} + 2N\varepsilon_{e\tau}^{dV}]^2$. It shows the degeneracy in the NSI parameters. As previously stated, targets with distinct N/Z could be used to break the degeneracy. Figure 8 shows the allowed region based on the combined analysis of results taking into consideration each

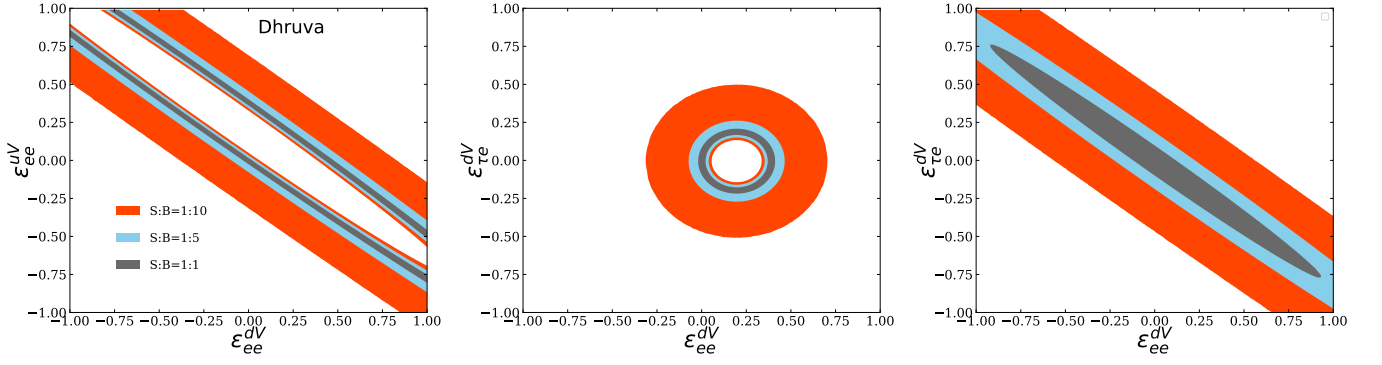


FIG. 10. Comparisons of sapphire detector sensitivity at 90% C.L. for different values of signal-to-background ratio.

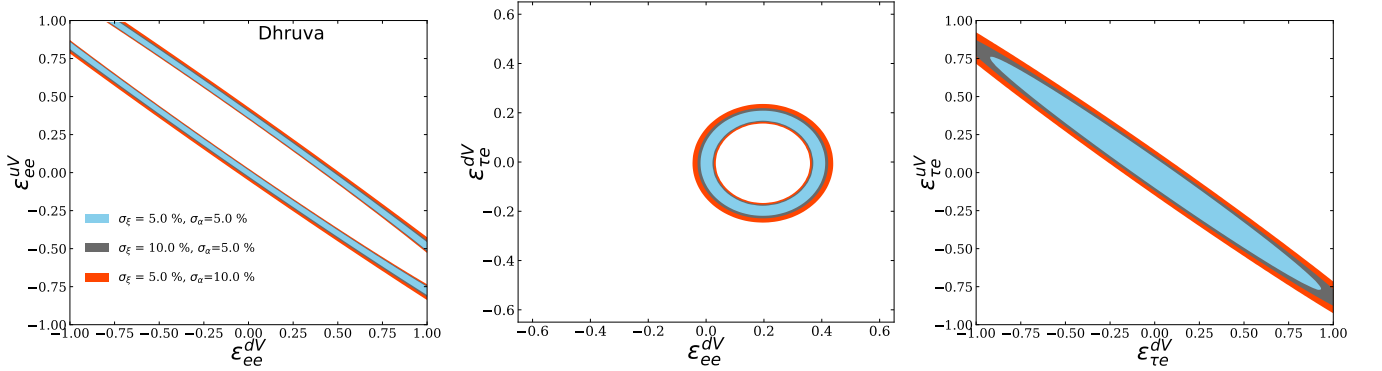


FIG. 11. Comparisons of sapphire detector sensitivity at 90% C.L. for different values of systematics. Results are extracted considering a signal-to-background ratio of one.

target of mass 5 kg of Al_2O_3 and Ge in the existence of background. Due to varying values of N and Z , it is found that the circle's center and radius differ for both detectors. It is observed that the combine result breaks the degeneracy, limits the allowed parameter space. Figure 9 shows the comparison on the sensitivity between expected results of the ICNSE sapphire detector and the COHERENT CsI detector [40]. It shows that the ICNSE detector can limit more parameter space compared to CsI detector of COHERENT experiment.

D. Effect of systematic and background on sensitivity

Studies have been carried out to find the impact of background and systematic considering the Dhruva reactor as a source for $\bar{\nu}_e s$ as there are several other basic science research are going on using neutron beam inside the reactor hall. Therefore, reactor related background is more at this site as compared to other facilities. In this case, it has been considered a sapphire detector of mass 10 kg placed at distance of 10 m from the Dhruva reactor core for an exposure of one year. It has been observed that the expected sensitivity of detector reduces with increase of background which is shown in Fig. 10. At 90% C.L., Fig. 11 shows the detector sensitivity to various NSI parameters considering different combination of systematic values. It is found that with increasing the value of σ_ξ

to 10.0% from 5.0%, the sensitivity of detector reduces. Further, for a given value of σ_ξ , by increasing the σ_α to 10.0% from 5.0% the sensitivity of the detector has been reduced more as compared to earlier case. So, it is necessary to reduce the background and related systematic uncertainty. Similarly, studies are carried out to find the detector sensitivity at various signal-to-background ratio for given values of σ_ξ (5.0%) and σ_α (5.0%). It can be noted here that further studies have been carried out considering a signal-to-background ratio of one and fixing the detector exposure.

E. Sensitivity to neutrino generalized interaction

The study has been carried out for an independent scalar interaction as well as a combination of scalar and vector interactions. The upper-left panel of Fig. 12 shows the 90% C.L. allowed regions in the $C_S^u - C_S^d$ plane, focusing primarily on scalar interactions. The contour is a single band due to minimal interference with the SM $CE\nu NS$ cross-section. The upper right panel shows the allowed contour region at 90% C.L. while considering both scalar and vector interactions. For simplicity, it has been assumed universal quark couplings, i.e., $C_S^u = C_S^d = C_S$ and $C_V^u = C_V^d = C_V$. The constrained region has a ring shape because of the interference effect from the vector interaction. The lower-left and lower-right panels

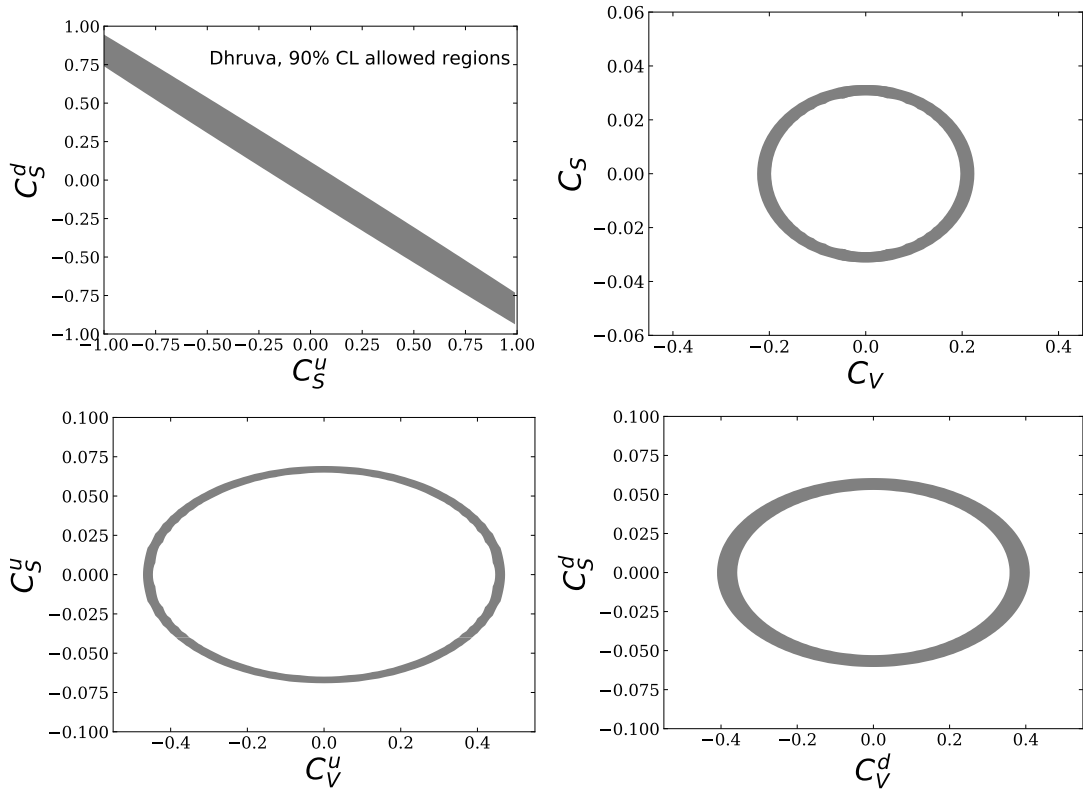


FIG. 12. The allowed regions on scalar and vector NGIs at 90% C.L. for a sapphire detector of mass 10 kg placed at 10 m from Dhruva reactor core. It has been considered a signal-to-background ratio of one and an exposure of one year.

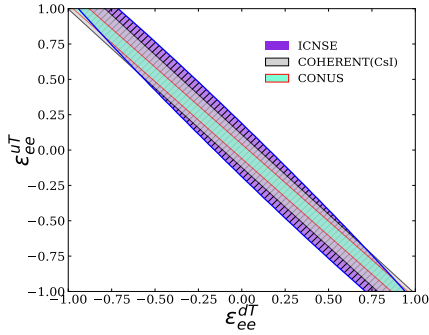


FIG. 13. An expected allowed regions of non-universal NSI tensor parameters $\epsilon_{ee}^{dT} - \epsilon_{ee}^{uT}$ plane at 90% C.L. considering detector made up of with Al_2O_3 . Result of the ICNSE detector has been extracted considering a signal-to-background ratio of one. Sensitivity at 90% C.L. due to COHERENT data has been taken form Ref. [6].

show results for scalar and vector interactions with u and d quarks only, respectively. As mentioned earlier, the NGIs involving d quarks are more constrained compared to those with u quarks, due to the neutron dominance in the $CE\nu NS$ cross section.

F. Sensitivity to non-universal NGI tensor parameters

In this analysis, the Dhruva reactor is utilized as a source of electron antineutrinos. Figure 13 illustrates the anticipated sensitivity to non-universal tensor NSI parameters in the $\epsilon_{ee}^{dT} - \epsilon_{ee}^{uT}$ plane at a 90% C.L. The constraints on the NSI tensor parameters are derived from the interactions of neutrinos with both u-type and d-type quarks. The observed behavior of these results can be explained through the arguments presented in the context of non-universal vector-type NSI interactions. Additionally, the figure also shows the comparison of detector sensitivity with others results such as an expected sensitivity of the CONUS [26] and the results obtained by analyzing the COHERENT data available in Ref. [6]. It has been found that sapphire detector can constrain most of the parameter space as like other experiments.

VI. SUMMARY

In this article, we explore the expected sensitivity reach of the ICNSE detector for constraining various parameters of nonstandard as well as generalized neutrino interactions using the coherent elastic neutrino-nucleus scattering process. The study has been performed considering an exposure of one year employing $\bar{\nu}_e$ s produced from a research reactor, which can be further employed for measurement at other available

power reactor. In the present study, high purity germanium and sapphire (Al_2O_3) detectors are considered. It is found that the detector can reach for constraining most of the NSI as well as NGI parameters space. The detector sensitivity is almost independent of reactor core. Further, there are degeneracies between different NSI parameters that appear while constraining more than one NSI parameter at a time using a single target. Results from a combination of two different types of detectors (Ge + Al_2O_3) having different neutron-to-proton ratios has one of the best sensitivities to the individual NSI parameters and can break the degeneracies between two NSI parameters for a large set of pairs of parameters. The expected sensitivity of the sapphire detector at a distance of 10 m from the reactor core are comparable with the other experiments and can put a stringent limit in the parameter space. The study also has been performed for with and without pres-

ence of background. The sensitivity deteriorates in presence of background noise. It has been observed that the detector has the potential for partially lifting these degeneracies when combining the results of two different detectors having different neutron to proton ratio. This study shows that the proposed neutrino experiment is sensitive to new physics of weak interaction and beyond. Finally, the sensitivity can be further improved by combining two different types of detectors with longer running time.

ACKNOWLEDGMENTS

The author would like to thank Avijit Bhattacharya and S. R. Sahu for his useful comments on the manuscript.

-
- [1] D. Z. Freedman, *Phys. Rev. D* **9**, 1389 (1974).
 - [2] D. Akimov *et al.* (COHERENT), *Science* **357**, 1123 (2017), [arXiv:1708.01294 \[nucl-ex\]](#).
 - [3] D. Akimov *et al.* (COHERENT), *Phys. Rev. Lett.* **129**, 081801 (2022), [arXiv:2110.07730 \[hep-ex\]](#).
 - [4] D. Akimov *et al.* (COHERENT), *Phys. Rev. Lett.* **126**, 012002 (2021), [arXiv:2003.10630 \[nucl-ex\]](#).
 - [5] S. Adamski *et al.* (COHERENT), (2024), [arXiv:2406.13806 \[hep-ex\]](#).
 - [6] D. K. Papoulias and T. S. Kosmas, *Phys. Rev. D* **97**, 033003 (2018), [arXiv:1711.09773 \[hep-ph\]](#).
 - [7] T. S. Kosmas, O. G. Miranda, D. K. Papoulias, M. Tortola, and J. W. F. Valle, *Phys. Rev. D* **92**, 013011 (2015), [arXiv:1505.03202 \[hep-ph\]](#).
 - [8] B. C. Cañas, E. A. Garcés, O. G. Miranda, and A. Parada, *Phys. Lett. B* **776**, 451 (2018), [arXiv:1708.09518 \[hep-ph\]](#).
 - [9] M. Atzori Corona, M. Cadeddu, N. Cargioli, F. Dordei, C. Giunti, and G. Masia, *Eur. Phys. J. C* **83**, 683 (2023), [arXiv:2303.09360 \[nucl-ex\]](#).
 - [10] M. Atzori Corona, M. Cadeddu, N. Cargioli, F. Dordei, and C. Giunti, (2025), [arXiv:2501.18550 \[hep-ph\]](#).
 - [11] M. Biassoni and C. Martinez, *Astropart. Phys.* **36**, 151 (2012), [arXiv:1110.3536 \[astro-ph.HE\]](#).
 - [12] V. Brdar, M. Lindner, and X.-J. Xu, *JCAP* **04**, 025 (2018), [arXiv:1802.02577 \[hep-ph\]](#).
 - [13] J. Colaresi, J. I. Collar, T. W. Hossbach, C. M. Lewis, and K. M. Yocum, *Phys. Rev. Lett.* **129**, 211802 (2022), [arXiv:2202.09672 \[hep-ex\]](#).
 - [14] N. Ackermann *et al.* (CONUS+), *Eur. Phys. J. C* **84**, 1265 (2024), [Erratum: *Eur.Phys.J.C* **85**, 19 (2025)], [arXiv:2407.11912 \[hep-ex\]](#).
 - [15] A. Aguilar-Arevalo *et al.* (CONNIE), *JHEP* **05**, 017 (2022), [arXiv:2110.13033 \[hep-ex\]](#).
 - [16] Z. Bo *et al.* (PandaX), *Phys. Rev. Lett.* **133**, 191001 (2024), [arXiv:2407.10892 \[hep-ex\]](#).
 - [17] E. Aprile *et al.* (XENON), *Phys. Rev. Lett.* **133**, 191002 (2024), [arXiv:2408.02877 \[nucl-ex\]](#).
 - [18] *Neutrino Non-Standard Interactions: A Status Report*, Vol. 2 (2019) [arXiv:1907.00991 \[hep-ph\]](#).
 - [19] S. Verma *et al.*, *Nucl. Instrum. Meth. A* **1046**, 167634 (2023), [arXiv:2203.15903 \[physics.ins-det\]](#).
 - [20] R. Strauss *et al.*, *Eur. Phys. J. C* **77**, 506 (2017), [arXiv:1704.04320 \[physics.ins-det\]](#).
 - [21] S. P. Behera, D. K. Mishra, P. K. Netrakanti, R. Sehgal, K. Kumar, R. Dey, and V. Jha, *Phys. Rev. D* **108**, 113002 (2023), [arXiv:2304.00912 \[hep-ph\]](#).
 - [22] S. P. Behera, (2025), [arXiv:2502.09972 \[hep-ph\]](#).
 - [23] K. Scholberg, *Phys. Rev. D* **73**, 033005 (2006).
 - [24] V. De Romeri, D. K. Papoulias, and G. Sanchez Garcia, *Phys. Rev. D* **111**, 075025 (2025), [arXiv:2501.17843 \[hep-ph\]](#).
 - [25] S. Navas *et al.* (Particle Data Group), *Phys. Rev. D* **110**, 030001 (2024).
 - [26] H. Bonet *et al.* (CONUS), *JHEP* **05**, 085 (2022), [arXiv:2110.02174 \[hep-ph\]](#).
 - [27] T. Singh, P. Pandey, T. Mazumdar, K. Singh, and V. Raina, *Annals of Nuclear Energy* **60**, 141 (2013).
 - [28] S. Agarwal, C. Karhadkar, A. Zope, and K. Singh, *Nuclear Engineering and Design* **236**, 747 (2006), india's Reactors: Past, Present, Future.
 - [29] S. Chetal, V. Balasubramanian, P. Chellapandi, P. Mohanakrishnan, P. Puthiyavinayagam, C. Pillai, S. Raghupathy, T. Shanmugham, and C. S. Pillai, *Nuclear Engineering and Design* **236**, 852 (2006), india's Reactors: Past, Present, Future.
 - [30] S. Agrawal, A. Chauhan, and A. Mishra, *Nuclear Engineering and Design* **236**, 812 (2006), india's Reactors: Past, Present, Future.
 - [31] P. Huber, *Phys. Rev. C* **84**, 024617 (2011), [Erratum: *Phys.Rev.C* **85**, 029901 (2012)], [arXiv:1106.0687 \[hep-ph\]](#).
 - [32] T. A. Mueller *et al.*, *Phys. Rev. C* **83**, 054615 (2011), [arXiv:1101.2663 \[hep-ex\]](#).
 - [33] H. T. Wong *et al.* (TEXONO), *Phys. Rev. D* **75**, 012001 (2007), [arXiv:hep-ex/0605006](#).
 - [34] M. Lindner, W. Rodejohann, and X.-J. Xu, *JHEP* **03**, 097 (2017), [arXiv:1612.04150 \[hep-ph\]](#).
 - [35] M. Bowen and P. Huber, *Phys. Rev. D* **102**, 053008 (2020), [arXiv:2005.10907 \[physics.ins-det\]](#).
 - [36] J. Barranco, O. G. Miranda, and T. I. Rashba, *JHEP* **12**, 021 (2005), [arXiv:hep-ph/0508299](#).
 - [37] E. Aprile *et al.* (XENON), *Phys. Rev. Lett.* **126**, 091301 (2021), [arXiv:2012.02846 \[hep-ex\]](#).
 - [38] J. Dorenbosch *et al.* (CHARM), *Phys. Lett. B* **180**, 303 (1986).
 - [39] S. Davidson, C. Pena-Garay, N. Rius, and A. Santamaria, *JHEP* **03**, 011 (2003).

- [40] J. Liao and D. Marfatia, [Phys. Lett. B **775**, 54 \(2017\), arXiv:1708.04255 \[hep-ph\]](#).